JCB

Article

Uncovering multiple axonal targeting pathways in hippocampal neurons

Dolora Wisco,[1] **Eric D. Anderson,**[2] **Michael C. Chang,**[1] **Caren Norden,**[1] **Tatiana Boiko,**[1] **Heike Fölsch,**[2] **and Bettina Winckler**[1]

[1]Brookdale Department of Molecular, Cell, and Developmental Biology, Mount Sinai School of Medicine, New York, NY 10029
[2]Department of Cell Biology, Yale Medical School, New Haven, CT 06520

Neuronal polarity is, at least in part, mediated by the differential sorting of membrane proteins to distinct domains, such as axons and somata/dendrites. We investigated the pathways underlying the subcellular targeting of NgCAM, a cell adhesion molecule residing on the axonal plasma membrane. Following transport of NgCAM kinetically, surprisingly we observed a transient appearance of NgCAM on the somatodendritic plasma membrane. Down-regulation of endocytosis resulted in loss of axonal accumulation of NgCAM, indicating that the axonal localization of NgCAM was dependent on endocytosis. Our data suggest the existence of a dendrite-to-axon transcytotic pathway to achieve axonal accumulation. NgCAM mutants with a point mutation in a crucial cytoplasmic tail motif (YRSL) are unable to access the transcytotic route. Instead, they were found to travel to the axon on a direct route. Therefore, our results suggest that multiple distinct pathways operate in hippocampal neurons to achieve axonal accumulation of membrane proteins.

Introduction

Cellular polarity is a fundamental property of most eukaryotic cells and is intricately linked to cellular function. One of the mechanisms underlying cell polarity is the differential sorting of membrane proteins to distinct plasma membrane domains on the biosynthetic route from the Golgi apparatus (Craig and Banker, 1994; Mellman, 1995; Winckler and Mellman, 1999). Polarized membrane traffic is best understood in epithelial cells, which have long served as the paradigm for similar studies in other mammalian cell types (Mellman, 1995; Mostov and Cardone, 1995; Folsch et al., 1999; Mostov et al., 2003). In the epithelial Madin-Darby canine kidney (MDCK) cell line, most membrane proteins destined for either the apical or basolateral domains are sorted directly in the TGN into two distinct vesicle populations (Wandinger-Ness et al., 1990). Not all epithelial cells use the TGN as the main sorting station for polarized cargo. In contrast to MDCK cells, another epithelial cell type, hepatocytes, transport almost all membrane proteins first to the basolateral surface. Only after internalization into endosomes does sorting of apical and basolateral membrane proteins take place. In hepatocytes then, apical proteins travel to the apical domain by an indirect, transcytotic pathway via the basolateral domain rather than on a direct route from the TGN (Tuma and Hubbard, 2003).

Much less is known about polarized membrane traffic in neurons. Dotti and Simons (1990) suggested that the apical domain of MDCK cells is equivalent to the axonal domain of cultured hippocampal neurons, and that the basolateral domain of MDCK cells is equivalent to the somatodendritic domain. This hypothesis was based on the observation that the basolateral vesicular stomatitis virus glycoprotein (VSVG) was sorted to the somatodendritic domain, and the apical influenza HA protein to the axonal domain. Therefore, the signals and the machineries recognizing them might be largely conserved between epithelial cells and cultured hippocampal neurons for apical/axonal and basolateral/somatodendritic transport. Indeed, transport of transmembrane proteins to the somatodendritic domain is mediated by cytoplasmic tail signals, which are frequently closely related to basolateral targeting determinants (West

Abbreviations used in this paper: BFA, brefeldin A; DIV, days in vitro; MDCK, Madin-Darby canine kidney; PI, polarity index.

Figure 1.   **NgCAM is found in somatodendritic endosomes positive for transferrin.** (A) Hippocampal neurons were infected with AdNgCAM for 24 h, fixed, and stained with a sandwich protocol to detect intracellular (red) and cell surface (green) pools of NgCAM. The axon is marked with arrows, dendrites with arrowheads. Single channel images of the boxed regions are shown in B (B1 and B2, axon; B3 and B4, dendrite). Intracellular NgCAM is red (B1 and B3) and cell surface NgCAM is green (B2 and B4). (C) Hippocampal neurons were infected with AdNgCAM for 24 h and incubated live with FITC–transferrin (green) for 30 min at 37°C before fixation. Cells were stained according to the sandwich protocol using anti-NgCAM antibodies and different secondary antibodies. Surface NgCAM was detected with a blue secondary Ab, showing axonal restriction of surface NgCAM (arrows mark the axon; this cell is bi-axonal). The axon appears magenta colored because of the overlap of blue and red. The internal NgCAM pool was detected with a red secondary Ab. (D) The insets show the soma region of the same cell processed with a thresholding program (Adobe Photoshop®) to show the simultaneous presence of transferrin (green; D1) and intracellular NgCAM (red; D2) in some endocytic compartments. Overlap appears yellow in D3. A representative, single confocal section is shown.
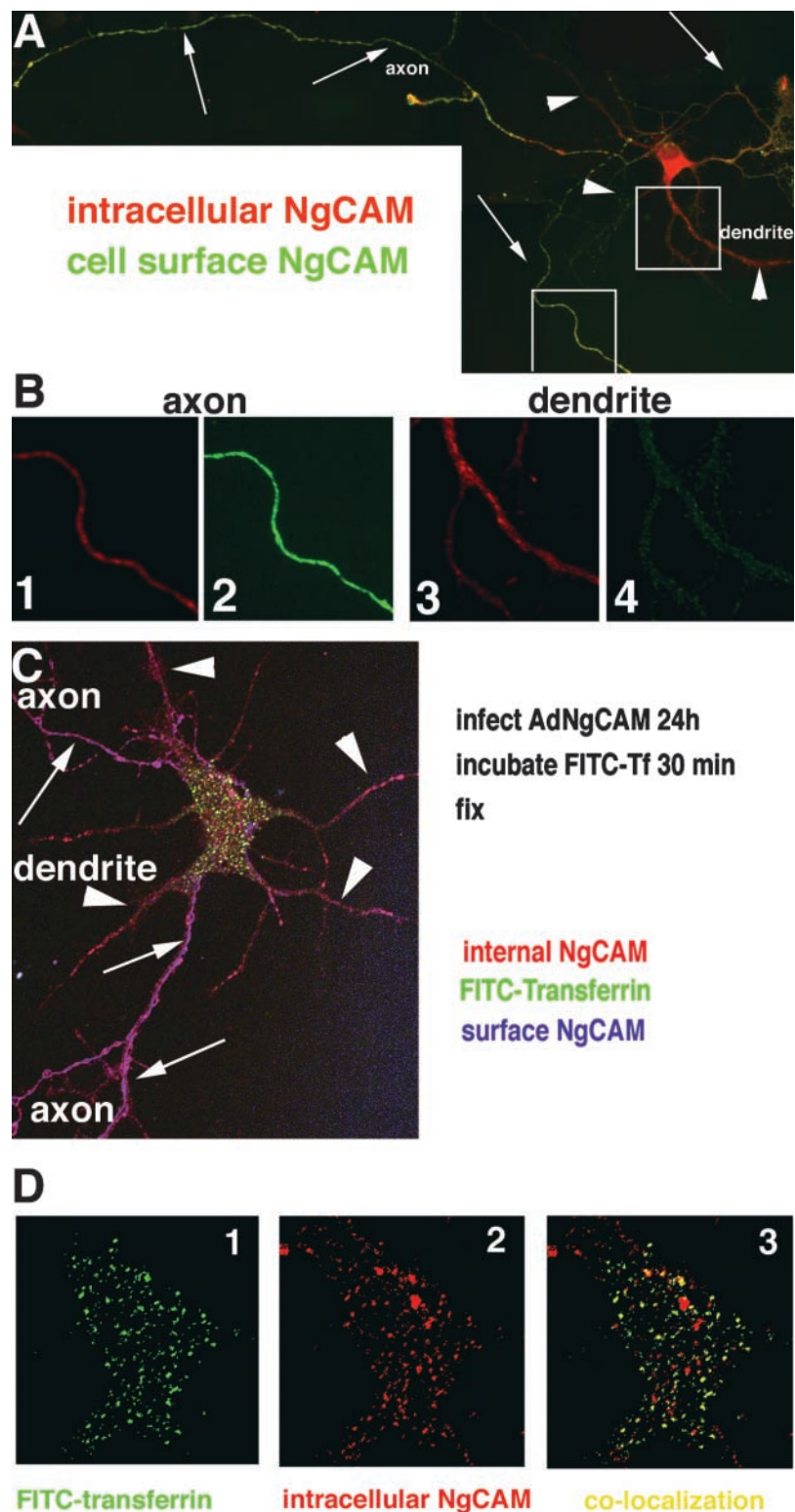
et al., 1997; Jareb and Banker, 1998; but see also Cheng et al., 2002).

Travel to the axon is less well understood (Winckler and Mellman, 1999) and might not be strictly conserved (Colman, 1999). Similarly to MDCK cells, extracellular/transmembrane domains are important for axonal targeting of at least some proteins (e.g., amyloid precursor protein [Tienari et al., 1996] and NgCAM [Sampo et al., 2003]). On the other hand, exog-

enously expressed apical proteins are often found uniformly on axons and dendrites rather than polarized to the axon (Jareb and Banker, 1998). In many studies, the interpretation of results is complex because exogenous expression of the protein leads to axonal localization, but the protein is additionally found brightly in all or part of the soma and dendrites (Jareb and Banker, 1998; Stowell and Craig, 1999; Francesconi and Duvoisin, 2002). Whether this reflects an inability of neurons
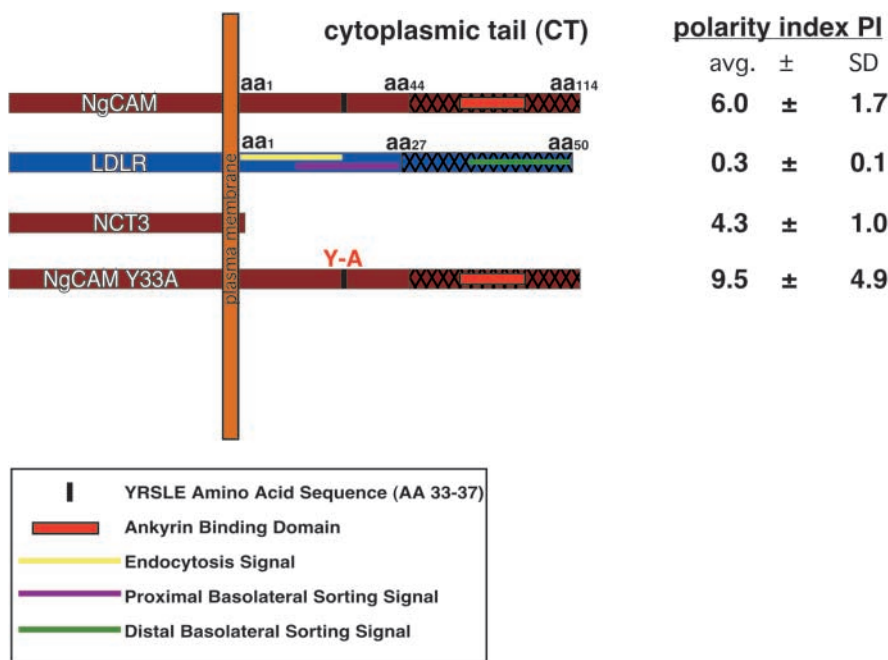
Figure 2.   **Quantification of axonal localization of NgCAM and NgCAM mutants.** NgCAM constructs are depicted as schematics. The 114-aa cytoplasmic tail of NgCAM is numbered from the first residue of the cytoplasmic tail, Lys_1. The ankyrin binding domain is indicated by an orange box. The YRLS motif is indicated by a black bar. A PI was determined as described in the Materials and methods by dividing the axonal by the dendritic average pixel intensities. Uniform staining gives a PI value of around 1. Preferential axonal staining gives a PI value of >1, whereas preferential somatodendritic enrichment gives a PI value of <1. The average PI (±SD) is indicated for wild-type NgCAM, the somatodendritic LDLR, and two NgCAM mutants, N(CT3) and NgCAM(Y33A).

to read and execute the same signals or is primarily due to missorting because of high overexpression is unclear.

In contrast, the axonal localization of the adhesion molecule NgCAM is preserved even upon exogenous overexpression in a high percentage of expressing neurons (Vogt et al., 1996; Jareb and Banker, 1998; Winckler et al., 1999). Therefore, the mechanisms underlying axonal targeting of NgCAM (the chick homologue of L1) have been investigated in several studies (Kamiguchi and Lemmon, 1998; Burack et al., 2000; Sampo et al., 2003). Experiments using live imaging of NgCAM–EGFP demonstrated that Ng-CAM–EGFP-containing intracellular vesicles are not polarized to axons but rather found well into dendrites as well as axons (Burack et al., 2000). Surface NgCAM at steady state, on the other hand, is highly enriched on the axonal surface and largely absent from the soma and dendrites. Based on these observations, Burack et al. (2000) proposed that transport of post-Golgi NgCAM-containing vesicles occurs nondiscriminately into both axons and dendrites, and that the polarized surface distribution arises from selective and preferential fusion of NgCAM vesicles with the axonal plasma membrane.

An alternative model for achieving steady-state axonal enrichment was proposed by Garrido et al. (2001) based on experiments with an axonally enriched voltage-gated sodium channel (VGNC) chimera. Axonal localization of VGNC chimeras was dependent on an endocytosis motif that mediated preferential internalization from the somatodendritic domain, thereby leading to net enrichment on the axonal surface. The axonal accumulation of VAMP2 was similarly dependent on an endocytosis signal (Sampo et al., 2003). Thus, VAMP2 might localize primarily to the axon because of preferential somatodendritic removal.

Recently, Sampo et al. (2003) further investigated the axonal targeting of NgCAM and found that NgCAM internalization from the somatodendritic surface was largely undetectable, except in a small subpopulation of cells. Therefore,

they proposed that NgCAM is sorted to the axon by selective axonal fusion and not by preferential somatodendritic removal. However, direct positive evidence supporting this model is still lacking, and many questions concerning the axonal trafficking pathway of NgCAM remain unanswered. In this work, we test these different models more directly by analyzing the transport pathways involved in axonal targeting of NgCAM kinetically. Our data suggest a model in which NgCAM can travel to the axon by a new pathway, i.e., via dendrite-to-axon transcytosis. Additionally, we found that signals required for the transcytotic pathway are encoded in NgCAM's cytoplasmic tail. Deletions of crucial regions in the cytoplasmic tail of NgCAM result in mutant proteins that are unable to access the transcytotic pathway and travel instead directly from the TGN to the axon. Our data suggest that hippocampal neurons possess both transcytotic and direct axonal sorting pathways.

Results

NgCAM is present in somatodendritic endosomes

Previously, intracellular organelles containing EGFP–Ng-CAM were found in dendrites and somata as well as axons at steady state (Burack et al., 2000). After infection of cells with a defective adenovirus encoding NgCAM (AdNg-CAM) for 24 h, we visualized internal and surface pools of NgCAM with different fluorophores using a sandwich protocol (Kamiguchi and Lemmon, 2000). We similarly find NgCAM in intracellular somatodendritic compartments (Fig. 1, A and B3) as well as in intracellular compartments in the axon (Fig. 1, A and B1). The surface pool of NgCAM, on the other hand, is highly enriched on the axon (Fig. 1, A, B2, and B4). Next, we quantified the extent of cell surface polarization of NgCAM using IP software to determine a "polarity index" (PI) similar to that used by others (Cheng et al., 2002; Sampo et al., 2003; see Materials and methods for details). Uniform staining gives a PI value of 1, whereas ax-

onal enrichment gives a PI value of >1, and somatodendritic enrichment gives a PI value of <1. For virally expressed NgCAM, the PI is 6.0, indicating sixfold axonal enrichment (Fig. 2).

We first wanted to test whether some of these somatodendritic compartments containing NgCAM are endosomes. To this end, we again infected cells with AdNgCAM for 24 h. Subsequently, live cells were incubated with FITC–transferrin for 30 min before fixation. Transferrin is a recycling ligand that is taken up into early and recycling endosomes but is largely excluded from late endosomes and lysosomes (Mellman, 1995). The cell surface and intracellular pools of NgCAM were differentially stained and analyzed by confocal fluorescence microscopy (Fig. 1 C). A subset of the intracellular vesicular profiles of NgCAM present in the somatodendritic domain colocalized with internalized transferrin (Fig. 1 D; yellow indicates overlap), suggesting that some of the somatodendritic compartments containing NgCAM are endosomes.

Next, we asked whether NgCAM reached these somatodendritic endosomes via the cell surface or by direct transport from the TGN. Thus, we assayed NgCAM uptake by incubating cells expressing NgCAM with antibodies to NgCAM's extracellular domain for 30 min before fixation. Cell surface and internalized antibodies were then differentially stained using the sandwich protocol with only secondary antibodies. We found that surface NgCAM was restricted to the axon (blue), while internalized anti-NgCAM antibodies (red) were detected in the somatodendritic domain in ~50% of NgCAM-expressing cells (Fig. 3, A and B). Uninfected control cells did not have detectable staining even after 2 h of incubation with anti-NgCAM antibodies, indicating that nonspecific uptake of antibodies was negligible (unpublished data).

To further characterize the compartments that accumulate internalized NgCAM, we incubated neurons infected with AdNgCAM with both anti-NgCAM antibodies and FITC–transferrin for 30 min before fixation. We find that internalized NgCAM colocalizes to a significant extent (>60% of profiles) with internalized FITC–transferrin (Fig. 3 B; yellow indicates overlap) in the soma. Taken together, these observations suggest that NgCAM on the cell surface can reach early/recycling endosomes in the somatodendritic membrane domain.

Inhibition of endocytosis disrupts axonal localization of NgCAM

Our observations raised the possibility that NgCAM is internalized from the somatodendritic domain. To test whether endocytosis was necessary for axonal accumulation of NgCAM, we down-regulated endocytosis by expressing a dominant-negative dynamin1(K44A) (Seeger and Payne, 1992; Damke et al., 1995; Schmid et al., 2000; Fourgeaud et al., 2003). The extent of down-regulation of endocytosis by dynamin(K44A) is dependent on its expression levels, so that in cells expressing low amounts of dynamin(K44A), endocytosis will be inhibited only partially, whereas in cells expressing large amounts of dynamin(K44A), endocytosis will be inhibited more completely. If NgCAM were directly inserted into the axonal plasma membrane, it would not a pri-
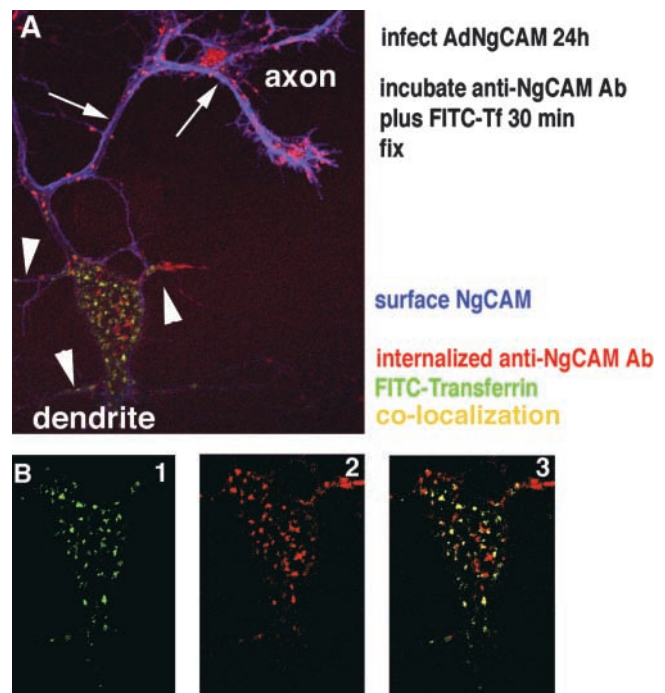

Figure 3. **NgCAM is internalized into a transferrin-positive somatodendritic compartment.** (A) Hippocampal neurons were infected with AdNgCAM for 24 h and incubated live with both FITC–transferrin (green) and anti-NgCAM antibodies for 30 min at 37°C before fixation. Cells were stained according to the sandwich protocol using only secondary antibodies. The surface-bound antibodies were detected with a Cy5-labeled secondary Ab (blue), showing axonal restriction of surface NgCAM (arrows mark the axon). Internalized antibodies were detected with Alexa®568-labeled secondary Ab (red). Internalized NgCAM (red) was detected in the axonal growth cone and along the axon (arrows) as well as in the soma. Uptake of FITC–transferrin can only be detected in the soma and dendrites (arrowheads). (B) Single channel images of the soma region of the same cell are shown processed with a thresholding program to show the simultaneous presence of transferrin (green; B1) and internalized NgCAM (red; B2) in some endocytic compartments. Overlap appears yellow in B3. A representative, single confocal section is shown.

ori depend on endocytosis for axonal localization and would therefore be expected to be unaffected by coexpression of dynamin(K44A). In contrast, if NgCAM had to be selectively removed from the somatodendritic surface for axonal accumulation, high levels of dynamin(K44A) expression would compromise axonal polarization.

Cells were infected with a recombinant adenovirus encoding dynamin(K44A) for several hours before either transfection with a plasmid encoding NgCAM or infection with AdNgCAM. Cells were fixed 20 h later and stained against surface NgCAM and internal dynamin(K44A). We observed a significant change in the distribution of NgCAM in cells expressing dynamin(K44A). A representative experiment is shown in Fig. 4 A. The percentage of cells that expressed NgCAM preferentially on the axonal surface decreased dramatically, while the proportion of uniformly expressing cells increased. This observation suggests that endocytosis is a necessary step for axonal accumulation of NgCAM. Surprisingly, we also observed a novel population of cells (~20%) expressing NgCAM primarily on the somatodendritic do-
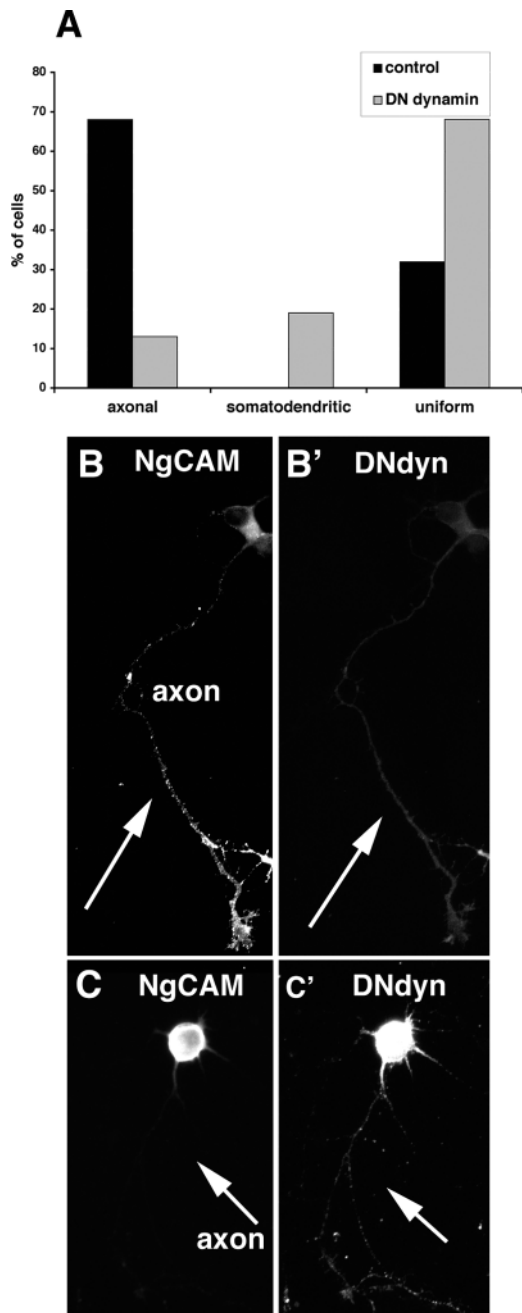
Figure 4.   **Inhibition of endocytosis leads to loss of axonal polarization of NgCAM.** (A) Neuronal cultures expressing NgCAM in the presence (gray bars; DNdynamin) or absence (black bars; control) of dominant-negative dynamin (DN-dynamin[K44A]) were stained, and the localization of NgCAM quantified. A representative experiment is shown. (B and B′) Example of a neuron expressing NgCAM (B) and low levels of DN-dynamin(K44A) (B′). NgCAM remains axonally enriched. (C and C′) Example of a neuron that expresses NgCAM (C) and high levels of DN-dynamin(K44A) (C′). NgCAM accumulates on soma and dendrites (arrowheads) and is largely absent from the axon (arrows).

main, i.e., showing reversed polarity (Fig. 4, C and C′). Furthermore, this population was only observed in cells expressing high levels of dynamin(K44A), but never in control cells. As is the case with dominant-negative approaches in general, the extent of inhibition is dependent on the expression level

of the dominant-negative protein. In accordance with this, we observe no effects of low levels of dynamin(K44A) on axonal localization of NgCAM (Fig. 4, B and B′). At high levels of dynamin(K44A) expression where endocytosis was most likely effectively blocked, NgCAM accumulated on the somatodendritic domain (Fig. 4, C and C′).

Following the transport kinetics of NgCAM

Our observation of somatodendritically enriched NgCAM raised the possibility that NgCAM is first targeted to the somatodendritic surface, reinternalized, and then transcytosed to the axon. We therefore decided to study the kinetics of NgCAM transport from the TGN to the plasma membrane. To this end, we applied a pulse-chase approach making use of the secretion inhibitor brefeldin A (BFA) (Chardin and McCormick, 1999). BFA is a highly specific blocker of Arf1-dependent membrane transport in both the Golgi and endosomes, and its effects are readily reversible in all cell types studied, including cultured hippocampal neurons (Craig and Banker, 1994; Cid-Arregui et al., 1995; Jareb and Banker, 1997). As retrograde Golgi transport is still active in the presence of BFA, Golgi membranes and associated proteins flow back into the ER, forming a hybrid ER/Golgi compartment (Klausner et al., 1992). Membrane proteins, including newly synthesized NgCAM, accumulate in the ER/Golgi compartment during BFA treatment and fail to reach the plasma membrane (unpublished data). As the BFA block is reversible, a wave of transport of the accumulated membrane proteins can be observed after removal of BFA (i.e., "pulse"). The progress of this pulse can be observed by fixing the cells after intervals following BFA washout (i.e., "chase").

We infected neuronal cultures with AdNgCAM for 4 h, treated overnight with BFA to stop Golgi trafficking, washed the BFA away, and fixed the cells at various intervals thereafter. Internal and surface pools of NgCAM were differentially stained as before. Strikingly, surface expression of NgCAM was first detectable on the somatodendritic domain, i.e., with reversed polarity (Fig. 5 A). Cells with somatodendritic NgCAM were also observed when the primary antibody was added to live cells (unpublished data) and then fixed, rather than after fixation without permeabilization. Indeed, 4 h after washing out BFA, 30% of infected cells expressed NgCAM with reversed polarity (Fig. 5 B, circles), while most of the rest (67%) showed only intracellular staining (Fig. 5 B, diamonds, stippled line). Of the cells with detectable surface expression at 4 h of chase, 92% show somatodendritic restriction of NgCAM. This somatodendritic pool could then be quantitatively chased to the axonal plasma membrane over time (Fig. 5 B, squares). These observations suggest that during biosynthetic transport from the Golgi, NgCAM is first inserted into the somatodendritic plasma membrane.

To corroborate this unexpected finding, an alternative pulse-chase assay was used that avoided the use of BFA. After infection with AdNgCAM, membrane traffic was arrested by incubating the cells at 19°C for 12 h (Scales et al., 1997). Subsequently, the cells were warmed to 37°C to allow membrane traffic to proceed ("pulse"), and then the cells were fixed at several time intervals after warming
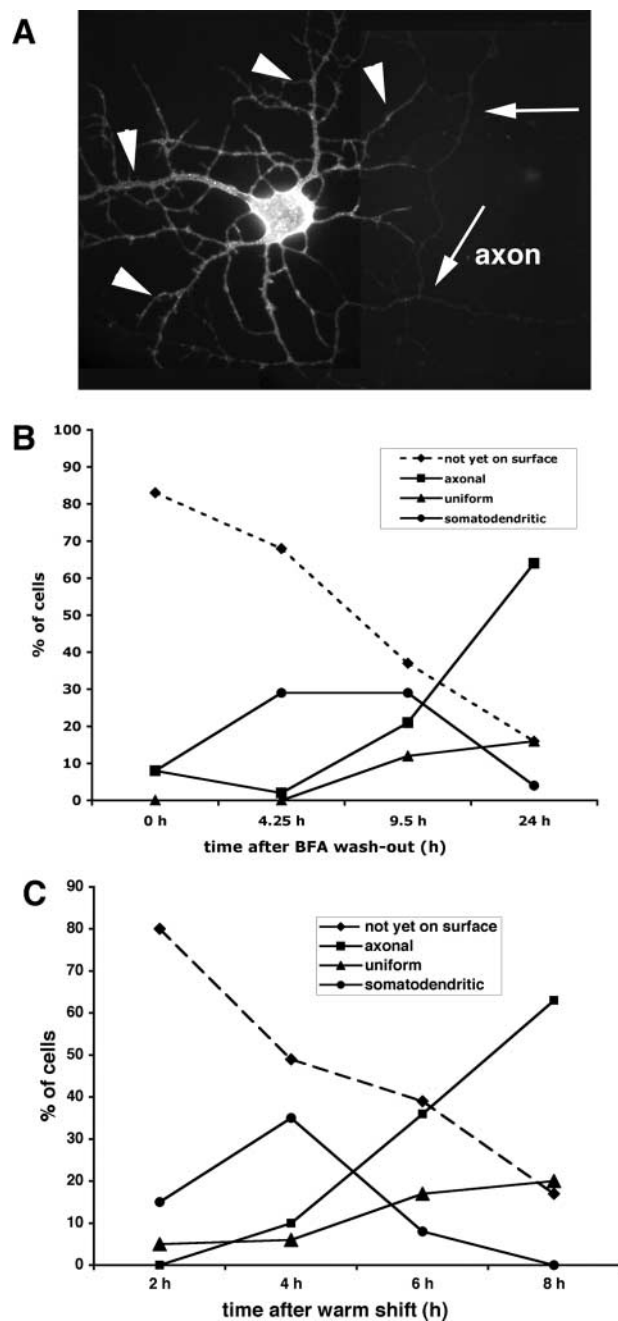
Figure 5. **Kinetic analysis of NgCAM transport reveals a somato-dendritic transport intermediate.** (A) After infection with AdNgCAM, NgCAM was accumulated in the ER/Golgi compartment by an overnight treatment with BFA. Transport of the accumulated membrane proteins was then followed after removal of BFA by fixation at different time points and immunostaining according to the sandwich method to distinguish between surface and internal NgCAM pools. A representative cell expressing NgCAM with somato-dendritic surface polarity 4 h after BFA washout is shown. The axon is marked by arrows, dendrites by arrowheads. (B) The appearance of the expressed proteins on the cell surface was counted (y axis) after BFA removal and scored as axonal (squares), uniform (triangles), or somatodendritic (circles). Cells with only internal staining were scored as not yet on surface (diamonds, stippled line). The quantitation of a representative experiment is shown. This experiment was repeated independently more than five times. (C) Cells were infected with AdNgCAM for 6 h, shifted to 19°C for 12 h, and then shifted back to 37°C for various amounts of time. The percentage of cells expressing NgCAM either not yet on the surface (diamonds, stippled

("chase"). We obtained qualitatively similar results with this second approach: after arrest of membrane traffic and subsequent release, NgCAM was first detected on the cell surface in the somatodendritic domain (Fig. 5 C). Again, this population could be chased to the axon over time. The kinetics of axonal appearance are somewhat faster after cold block release than after BFA block release. This is likely an indication that the Golgi block is more readily reversed after cold treatment than after BFA treatment, resulting in a tighter chase of NgCAM to the surface.

We also wanted to see if we could detect somatodendritic NgCAM without using any TGN transport block. Therefore, we fixed and stained AdNgCAM-infected cells at early time points after infection (21 h), when NgCAM first appeared at the cell surface. Surface expression was low at this point, and only ∼25% of infected neurons had any detectable surface expression at all. We could detect a small percentage of cells with somatodendritic enrichment of Ng-CAM (unpublished data). We therefore consider it unlikely that the initial somatodendritic surface appearance is an artifact caused by the use of BFA. Rather, our kinetic data suggest that NgCAM first appears at the somatodendritic surface and not at the axonal membrane domain.

Furthermore, quantitative analysis of multiple cells at short times after BFA release with IP software showed that in cells with "somatodendritic/reversed polarity" (Fig. 5 B, circles), >80% of the fluorescence signal is on the somatodendritic domain. The initial somatodendritic delivery therefore appears to be the predominant pathway followed by the majority of NgCAM molecules leaving the TGN and not a minor salvage pathway traveled by only a small percentage of missorted molecules. Based on these findings, we propose the following model for NgCAM delivery to the axon: (1) NgCAM travels from the TGN primarily to the somatodendritic plasma membrane, (2) the protein is internalized, and (3) NgCAM traffics from somatodendritic endosomes to the axonal plasma membrane by transcytosis.

Direct and indirect axonal pathways exist

We next sought to determine the regions of NgCAM that contain the trafficking signals necessary for transcytosis. Numerous studies have demonstrated that the cytoplasmic tail of NgCAM contains signals important for trafficking and localization of the molecule (Kamiguchi and Lemmon, 1998; Kamiguchi et al., 1998). Thus we generated a truncated NgCAM construct, NgCAM(CT3), lacking all but three amino acids of its cytoplasmic tail (Fig. 2). Neuronal cultures were simultaneously infected with AdNgCAM(CT3) and Adp75NGFR. P75NGFR is present on both axons and dendrites and serves to visualize both axonal and somatodendritic domains (Fig. 6 A, inset). We found that NgCAM(CT3) is axonally enriched at steady state (Fig. 2; Fig. 6 A), indicating that axonal targeting information is encoded in NgCAM's ectodomain (Sampo et al., 2003).

line), axonal (squares), uniform (triangles), or somatodendritic (circles) was determined. A transient somatodendritic population was observed at short times after the chase. At longer chase times, NgCAM accumulated in the axon.

To analyze whether NgCAM(CT3) still reaches the axonal membrane via transcytosis, we studied the transport kinetics of NgCAM(CT3) using the BFA pulse-chase assay. In contrast to full-length NgCAM, NgCAM(CT3) was never detected on the somatodendritic surface (circles) after BFA washout (Fig. 6 B). We first detected surface expression after 2 h of chase. Even at these earliest times of detectable surface expression, NgCAM(CT3) was already axonally enriched on the plasma membrane (Fig. 6 B, squares). Therefore, Ng-CAM(CT3) appears to be directly delivered from the TGN to the axonal plasma membrane. Therefore, both direct and transcytotic axonal pathways exist.

The initial somatodendritic delivery of NgCAM requires the $Y_{33}RSL$ motif

Next, we asked which cytoplasmic tail sequences of NgCAM are required for the initial somatodendritic insertion. Previously, the $Y_{33}RSL$ motif has been demonstrated to control endocytosis of NgCAM through its interaction with the clathrin adaptor complex AP-2 (Kamiguchi et al., 1998). Interestingly, tyrosine-based endocytosis signals are sometimes colinear with tyrosine-based basolateral and/or somatodendritic sorting signals (Matter et al., 1992, 1993, 1994).

To test the idea that the $Y_{33}RSL$ motif might be needed for initial somatodendritic targeting before endocytosis, we generated a recombinant construct, NgCAM(Y33A), in which the $Y_{33}RSL$ motif was disrupted by mutating tyrosine$_{33}$ to alanine (Fig. 2). Again, neuronal cultures were simultaneously infected with Adp75NGFR to visualize all processes (Fig. 7 B). We found that NgCAM(Y33A) was well polarized to the axon at steady state (Fig. 2; Fig. 7, A and B). To determine how NgCAM(Y33A) arrived at the axon, we used the BFA pulse-chase assay. Similarly to NgCAM(CT3), Ng-CAM(Y33A) was enriched on the axonal plasma membrane (Fig. 7 C, squares) even at the earliest times of detectable surface expression. No somatodendritic population was ever observed, suggesting transport via a direct pathway.

Transport along a direct pathway is expected to be independent of endocytosis. We, therefore, tested whether down-regulation of endocytosis would affect the axonal localization of NgCAM(Y33A) by coexpressing dynamin (K44A) and NgCAM(Y33A). We found that axonal localization of NgCAM(Y33A) was unaffected by coexpression of dynamin(K44A) (Fig. 7 D), and therefore appeared independent of endocytosis, consistent with direct routing to the axon. Therefore, these data suggest that a mutation in the $Y_{33}RSL$ motif prevents the initial somatodendritic delivery of NgCAM and changes the axonal transport pathway from transcytotic to direct. Therefore, the $Y_{33}RSL$ motif might serve as a somatodendritic targeting determinant facilitating the sorting of NgCAM at the TGN.

Discussion

A transcytotic model for NgCAM transport to the axon

The pathways and molecular mechanisms underlying polarized membrane traffic in neurons are not well understood. Several possible pathways for axonal enrichment of membrane proteins have been proposed, among them selective fusion with the axonal membrane (Sampo et al., 2003) or se-
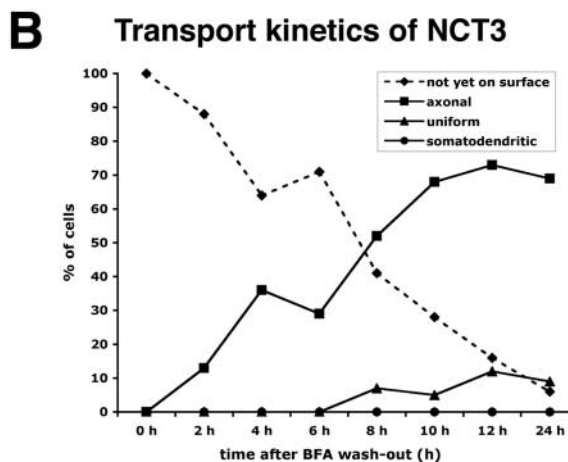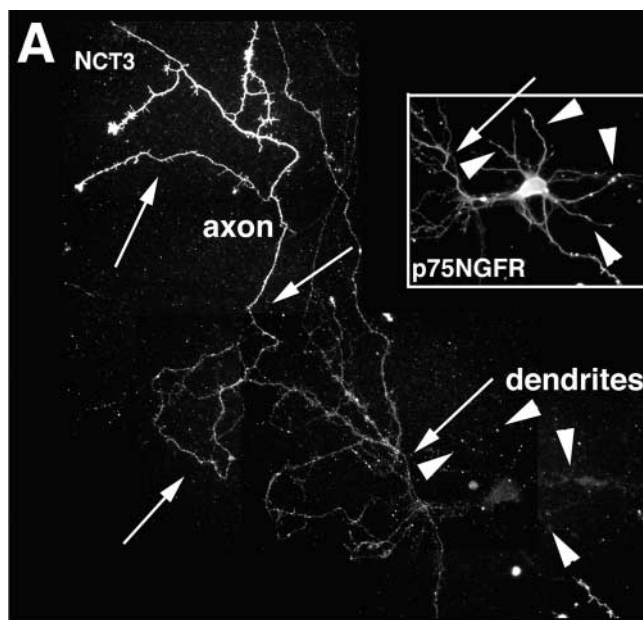

Figure 6. **The cytoplasmic tail of NgCAM is required for transcytotic delivery to the axon.** (A) Hippocampal neurons 8–10 DIV were infected with recombinant adenoviruses expressing NgCAM(CT3) for 30 h, fixed, and stained with mouse monoclonal antibodies against the extracellular domain of the virally expressed protein and detected with Alexa®488-labeled goat anti–mouse secondary antibodies. To delineate all processes (soma region shown in inset), all cells were simultaneously infected with Adp75NGFR. Axons are marked with arrows, dendrites with arrowheads. (B) Transport kinetics of NgCAM(CT3) using the BFA block/release assay (see Fig. 4 legend). NgCAM(CT3) appears directly on the axonal surface.

lective removal from the somatodendritic domain (Garrido et al., 2001). To determine how NgCAM travels to the axon, we carefully investigated its trafficking pathway from the TGN to the plasma membrane. Based on our findings, we propose that NgCAM first inserts into the somatodendritic domain (1) and, after endocytosis, (2) reaches somatodendritic early/recycling endosomes before the molecule travels to the axon via transcytosis (3) (Fig. 8).

This model is based on the following evidence. When we followed a pulse of NgCAM molecules leaving the TGN after a block with BFA or low temperatures, we observed ini-
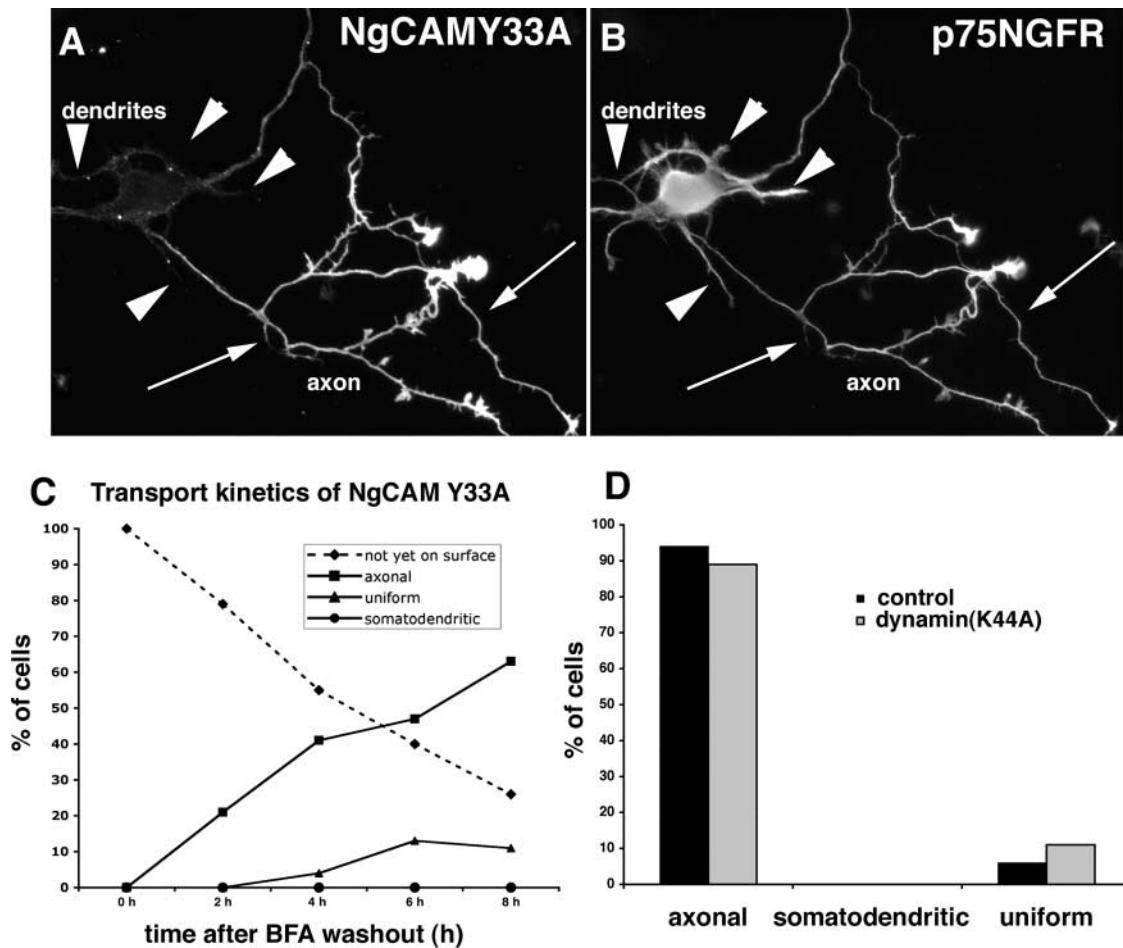
Figure 7. **The YRSL motif is required for transcytosis.** Neurons (8–10 DIV) were coinfected with AdNgCAM(Y33A) (A) and defective adenoviruses encoding the uniformly expressed p75/NGFR (B) for 30 h. NgCAM(Y33A) is axonally enriched (arrows mark axon, arrowheads mark dendrites). (C) Transport kinetics of NgCAM(Y33A) using the BFA block/release assay (see Fig. 4 legend). NgCAM(Y33A) appears directly on the axonal surface. (D) Quantitation of NgCAM(Y33A) polarization in neurons that are (gray bars; DNdynamin) or are not (black bars; control) expressing dominant-negative dynamin(K44A). A representative experiment is shown.

tial appearance on the cell surface preferentially in the somatodendritic domain (Fig. 5). Furthermore, when endocytosis was inhibited through overexpression of dominant-negative dynamin1(K44A), axonal accumulation of NgCAM was significantly blocked (Fig. 4). In cells expressing high levels of dynamin1(K44A), NgCAM even accumulated at the somatodendritic domain instead. If however endocytosis was not blocked, we detected internalized NgCAM in somatodendritic early or recycling endosomes where it partially colocalized with internalized transferrin (Fig. 3). At later time points after the release of a TGN exit block, NgCAM was chased to the axon (Fig. 5).

Multiple signals are required for transcytosis

NgCAM contains all the signals needed for a transcytotic pathway: a somatodendritic and endocytosis signal colinear with YRSL and an axonal targeting determinant in the extracellular domain. To traverse a transcytotic pathway, these signals presumably need to be read and executed sequentially in different intracellular compartments: the somatodendritic signal in the TGN, the endocytosis signal on the plasma membrane, and the axonal signal in the endosome. How

cells accomplish this kind of hierarchical read-out of multiple signals is not well understood for any protein. The best-studied receptor undergoing transcytosis is the pIgR, which carries dimeric IgA from the basolateral to the apical side of epithelial cells (Mostov and Cardone, 1995). For pIgR, ligand binding stimulates transcytosis several-fold in epithelial cells (van Ijzendoorn et al., 2002). The same was found for neurons (de Hoop et al., 1995). It has been suggested that phosphorylation of a serine residue in the basolateral sorting motif silences it and permits apical delivery from endosomes (Casanova et al., 1990; Luton et al., 1998).

The molecular mechanisms underlying the transcytotic pathway of NgCAM in neurons await further studies. In epithelial cells, NgCAM is enriched on the apical domain, which it reaches also via transcytosis (unpublished data). Here, sorting from the TGN to the basolateral membrane domain is dependent on the clathrin adaptor AP-1B and the sequence $Y_{33}RSL$ (unpublished data). However, as the adaptor complex AP-1B is not expressed in brain (Ohno et al., 1999), another protein might be required for the somatodendritic sorting step of NgCAM in neurons. In neurons, the disruption of the YRSL motif in NgCAM(Y33A) results
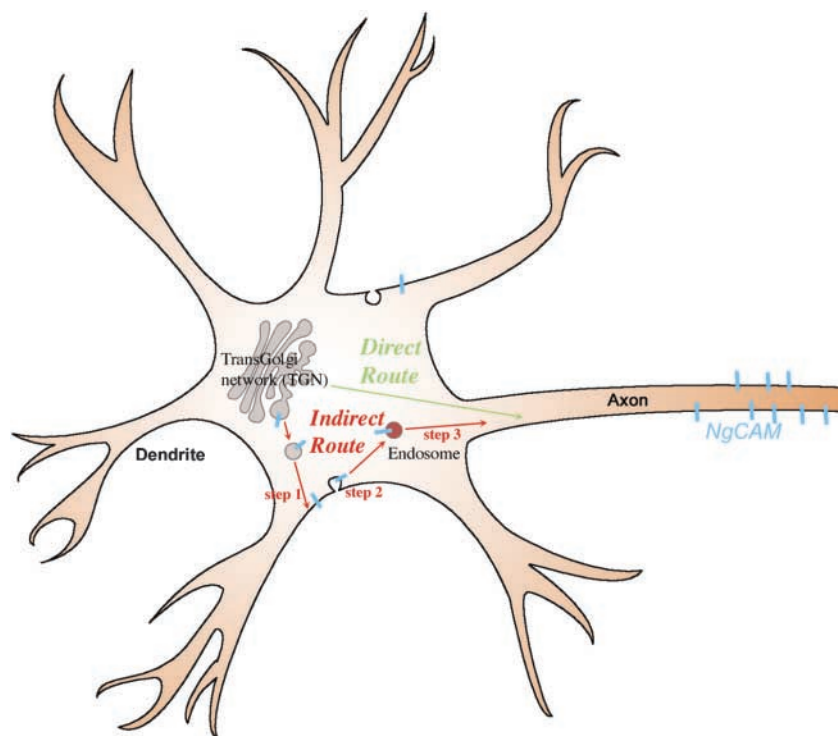
Figure 8.   **A model for axonal transport of NgCAM.** NgCAM (blue bars) travels on an indirect transcytotic route from the TGN (located in the soma) to the axon. The transcytotic indirect route consists of at least three steps: (1) TGN to somatodendritic plasma membrane, (2) somatodendritic plasma membrane to endosomes, and (3) endosome to axonal plasma membrane. Endocytosis is a necessary step for axonal delivery of NgCAM in this model.

in a mutant protein that now travels on a direct route and not via transcytosis (Fig. 7). This suggests that when the YRSL motif is present, the axonal targeting information contained within NgCAM's ectodomain cannot be executed in the TGN. How is the somatodendritic sorting signal silenced subsequently in the endosome to allow for axonal delivery of the full-length protein? Recently, Schaefer et al. (2002) demonstrated that the YRSL motif can be phosphorylated by src, which inhibits AP-2 binding. Such a phosphorylation event might similarly inhibit binding of other sorting adaptors, such as AP-1B. The YRSL motif might also bind to additional proteins (Dickson et al., 2002) whose interactions might be regulated by phosphorylation. Therefore, the phosphorylation of YRSL may silence its somatodendritic sorting information, allowing the phosphorylated protein to travel to the axon instead.

A different model for axonal transport of NgCAM has been proposed recently (Sampo et al., 2003). Sampo et al. (2003) tested whether NgCAM's polarization to the axonal plasma membrane arises from axonally restricted fusion of NgCAM-containing vesicles by assaying somatodendritic endocytosis of anti-NgCAM antibodies. Somatodendritic endocytosis of NgCAM could be observed, but only in a small subpopulation of neurons. The neurons with detectable somatodendritic endocytosis of NgCAM were described as looking less mature (Sampo et al., 2003). We similarly detected somatodendritic endocytosis of NgCAM, albeit in a very substantial proportion of the neurons ($\sim$50%). Why is somatodendritic endocytosis not seen in all neurons? Somatodendritic uptake might still take place in those cells but not be readily detectable. We did not notice any obvious correlation between cells with detectable somatodendritic endocytosis and axonal lengths, which might have indicated that different pathways operate in immature and mature

cells. Rather, it appeared to us that somatodendritic endocytosis was more readily detectable in cells with higher levels of NgCAM on the axonal surface. Low levels of newly synthesized NgCAM, and thus low levels of NgCAM on the somatodendritic surface at steady-state, and/or more rapid endocytic flux might account for the population of cells in which somatodendritic endocytosis was undetectable.

In our kinetic assays, we observe >90% of expressing neurons trafficking NgCAM via the somatodendritic surface. We therefore consider it likely that the relatively high proportion of neurons where somatodendritic endocytosis is undetectable can be attributed to technical limitations of the sensitivity of detection rather than to pathway heterogeneity in different neuronal populations. However, we cannot at this point completely rule out the possibility that different populations of cells, either less mature or of a different neuronal cell type, traffic NgCAM by distinct pathways to the axon. This could be regulated, for example, by differential phosphorylation of NgCAM's YRSL motif or some other mechanism and lead to developmental or cell type–specific regulation of pathway choice. More work needs to be done to explore these potentially exciting possibilities.

The cytoplasmic YRSL sequence has previously been identified as an axonal targeting motif of L1/NgCAM. Kamiguchi and Lemmon (1998) found that mutations in the YRSL motif lead to an accumulation of L1 in neurites of dorsal root ganglion neurons (rather than just somata). In hippocampal neurons, however, NgCAM with a mutation in the YRSLE motif did not accumulate in dendrites but was instead routed directly into the axon (Fig. 7). These observations raise the interesting possibility that different neurons may differ in the ways they process sorting signals of membrane proteins. Dorsal root ganglion neurons may sort all membrane proteins by default from the TGN to the soma-

todendritic domain and sort axonal and somatodendritic proteins away from each other only in the endocytic system, as is the case for hepatocytes. In contrast, hippocampal neurons, like MDCK cells, possess the ability to sort newly synthesized proteins already in the TGN.

Multiple pathways to the axons

Whether the majority of axonal membrane proteins travel to the axon primarily by a direct, a transcytotic, or a preferential retrieval pathway requires the study of more axonal proteins. Given that NgCAM travels transcytotically to the apical domain in MDCK cells (unpublished data), a minor pathway for apical proteins in MDCK cells, it is possible that most axonal proteins do not follow a transcytotic pathway in neurons. Could the transcytotic routing of Ng-CAM be of physiological significance? Interestingly, analysis of L1 knockout mice uncovered morphological abnormalities in the dendrites of some neuronal populations (Demyanenko et al., 1999). Therefore our discovery that a transcytotic pathway exists for NgCAM might be physiologically relevant, and the transient appearance of L1/Ng-CAM on the dendritic surface might play an important functional role.

Materials and methods

Reagents

The following adenoviruses were provided: AdNgCAM by P. Sonderegger (ETH Zurich, Zurich, Switzerland), AdHA-dynamin(K44A) by J. Pessin (University of Iowa, Iowa City, IA), and Adp75NGFR by M. Chao (New York University Medical School, New York, NY). The following antibodies were used: anti-NgCAM monoclonal antibody 8D9 from National Institutes of Health (NIH) hybridoma bank and anti-HA monoclonal antibody HA.11 from Babco. Rabbit antibody 9992 against the intracellular domain of p75NGFR was provided by M. Chao. FITC–transferrin and Alexa®-conjugated secondary antibodies were from Molecular Probes. Cy3-, Cy5-, and RRX-conjugated and unconjugated Fab fragments and IgGs were from Jackson ImmunoResearch Laboratories. BFA was from Epicentre Technologies.

Cell culture

Hippocampal cultures were prepared essentially as previously described (Winckler et al., 1999). In brief, embryonic day 18 rat hippocampi were dissected, dissociated by trituration after trypsin digestion, and plated on polylysine-coated coverslips. After 4 h, the cells were transferred into serum-free medium supplemented with B27 (GIBCO BRL) and cultured for 8–12 d. 293 cells were grown in DME with 10% FCS and 1% glutamine for adenoviral production.

Construction of adenoviral vectors

The gene encoding full-length NgCAM (variant) (GenBank/EMBL/DDBJ accession no. Z75013) was provided by P. Sonderegger. To generate Ng-CAM truncations, this gene was amplified by PCR using the oligonucleotides NgC25 (5′–GCGC**CTCGAG**ATGGCTCTGCCCCATGGG-3′) and NgC17 (5′–CGCG**TCTAGA**TTAATCCAGGGGGGGGCCC-3′), and cloned into the pCR-XL-TOPO vector of the Invitrogen TOPO® XL PCR Cloning Kit according to the manufacturer's instructions. The gene was then subcloned into the mutagenesis and expression vector pAlter-MAX (Promega) using the introduced XhoI and XbaI sites. The NgCAM truncation CT3 was generated by single-primer mutagenesis according to the manufacturer's instructions using the oligonucleotides CT3 (5′-GTCCTTCACCGAATA-CTTGCCCCC**TCTAGA**TTAGCTGCGTTTGATGAAGCAGAGGATG-3′) and Y33A (5′-CTCCTCCGCTTCGCTCTCCAACGACCTGGCCTCCCCAAAG-GTCTCATCCTTCATGGGCC-3′). The mutagenized constructs were cloned into the pShuttleCMV vector using the introduced XhoI and XbaI sites. Recombinant adenoviruses were subsequently generated using the AdEasy system from Qbiogene according to the manufacturer's instructions. In all oligonucleotides shown, the sequences complementary to the NgCAM sequence are underlined, and introduced restriction sites are shown in bold.

Adenoviral infection

Hippocampal cultures grown on glass coverslips were moved to 12-well plates in 500 μl conditioned medium in the presence of 1 mM kynurenic acid, and 1–5 μl of purified adenovirus was added per well. After 4 h, 500 μl of conditioned medium was added, and cells were incubated for 24–36 h. As we use the same antibodies to detect the expressed proteins, we note that the range of staining intensities found in a population of expressing neurons is comparable between different constructs.

BFA block/release

Cells were infected as described above. After 4 h, BFA (Epicentre Technologies) was added to 0.5–0.75 μg/ml final concentration. After 12–18 h, coverslips were washed twice in conditioned medium and transferred to fresh dishes. Coverslips were removed and fixed at indicated times and stained by the sandwich technique described below. The sandwich staining allowed counting of cells that were infected (i.e., positive for intracellular NgCAM) but where the protein had not reached the surface yet (i.e., negative for surface staining). We observe that the kinetics of surface transport are somewhat variable between cultures and appear slower for older cultures (12 days in vitro [DIV]) than for younger (8 DIV). All experiments were performed at least three independent times.

Immunofluorescence

Cells were fixed in 2% paraformaldehyde/3% sucrose/PBS in 50% conditioned medium at room temperature for 30 min and quenched in 10 mM glycine/PBS for 10 min. Alternatively, 2% paraformaldehyde/3% sucrose/0.125% glutaraldehyde/PBS was used in some experiments. The fixation conditions used do not introduce holes into most cells (not depicted). Coverslips were then blocked in 5% horse serum/1% BSA/PBS in the presence or absence of 0.05% saponin for 30 min. Antibodies were diluted in 1% BSA/PBS with or without 0.05% saponin and incubated for 1–2 h. Coverslips were mounted in Vectashield (Vector labs) and viewed on a Carl Zeiss MicroImaging, Inc. Axiophot with a 40× objective. Images were captured with the Orca cooled CCD camera (Hamamatsu) using Openlab software (ImproVision) and processed identically in Adobe Photoshop®. For surface staining, live cells were incubated for 5 min at room temperature in primary antibody before fixation and incubation with secondary antibodies.

Quantification of polarized distribution

Localization was quantified essentially as published elsewhere (Sampo et al., 2003). In brief, lines were traced along multiple segments of axons (8–10 segments covering most of the axon) and dendrites (along entire lengths of each dendrite), and average pixel intensities were determined along the traced lines. The intensities of all axonal and all dendritic segments were averaged. The average background intensity of uninfected cells was determined and subtracted from the axonal and dendritic intensity values. A PI was calculated by dividing the axonal by the dendritic average pixel intensities. Uniform staining gives a PI value of around 1. Preferential axonal staining gives a PI value of >1, whereas preferential somatodendritic enrichment gives a PI value of <1. The PI of 5–10 cells was determined for each construct and averaged.

Sandwich staining

To visualize the internal and surface population of NgCAM separately, a protocol similar to that published by Kamiguchi and Lemmon (2000) was used with modifications. In brief, cells were fixed, blocked, and incubated with primary antibody as described above. The primary antibody was detected with FITC–GαM Fab fragments (Jackson ImmunoResearch Laboratories). Any unbound primary antibodies were subsequently blocked with unconjugated GαM Fab fragments (1 mg/ml) for 1 h to overnight and fixed for 10 min. Cells were then permeabilized in 0.05% saponin/1% BSA/PBS for 30 min and incubated with a second round of primary antibodies. This second round of antibodies was detected with rhodamine red–labeled goat anti–mouse secondary antibodies (Jackson ImmunoResearch Laboratories). This protocol leads to separable staining of internal and external populations in all cells except very highly overexpressing cells. In those cases, the surface could not be completely blocked with unconjugated Fab fragments even at much higher concentrations.

Endocytosis assay

Cells were incubated in transferrin-free medium (Bottenstein and Sato N2.1 medium minus transferrin) for 1 h. FITC–transferrin (Molecular Probes) at 0.2 mg/ml was added simultaneously with anti-NgCAM antibodies (0.3 mg/ml) for 30 min at 37°C. After fixation, surface and internalized NgCAM were visualized using the sandwich protocol, except primary

antibody was omitted. Images were taken on a Leica TCS-SP confocal microscope. Uptake of antibody was mediated specifically by the virally expressed receptor molecules, as uninfected cells show no uptake even after 2 h of incubation with anti-NgCAM antibodies. The 8D9 antibody does not detect the endogenous rat L1. Binding of antibodies to live cells can in some cases cause either inhibition of endocytosis or transport to lysosomes. Neither is the case for NgCAM expressed in hippocampal neurons (not depicted). To determine overlap of internalized NgCAM and FITC–transferrin, a threshold function was applied in Adobe Photoshop®. For each channel, the threshold level was chosen such that very small and very faint puncta disappeared. Our procedure erred on the side of underestimating overlap between the two tracers. All pixel intensities above this threshold level were set to 255.

References

Burack, M.A., M.A. Silverman, and G. Banker. 2000. The role of selective transport in neuronal protein sorting. *Neuron.* 26:465–472.

Casanova, J.E., E.E. Breitfeld, S.A. Ross, and K.E. Mostov. 1990. Phosphorylation of the polymeric immunoglobulin receptor required for its efficient transcytosis. *Science.* 248:742–745.

Chardin, P., and F. McCormick. 1999. Brefeldin A: the advantage of being uncompetitive. *Cell.* 97:153–155.

Cheng, C., G. Glover, G. Banker, and S.G. Amara. 2002. A novel sorting motif in the glutamate transporter excitatory amino acid transporter 3 directs its targeting in Madin-Darby canine kidney cells and hippocampal neurons. *J. Neurosci.* 22:10643–10652.

Cid-Arregui, A., R.G. Parton, K. Simons, and C.G. Dotti. 1995. Nocodazole-dependent transport, and brefeldin A-sensitive processing and sorting, of newly synthesized membrane proteins in cultured neurons. *J. Neurosci.* 15:4259–4269.

Colman, D.R. 1999. Neuronal polarity and the epithelial metaphor. *Neuron.* 23:649–651.

Craig, A.M., and G. Banker. 1994. Neuronal polarity. *Annu. Rev. Neurosci.* 17:267–310.

Damke, H., S. Freundlieb, M. Gossen, H. Bujard, and S.L. Schmid. 1995. Tightly regulated and inducible expression of a dominant interfering dynamin mutant in stably transformed HeLa cells. *Methods Enzymol.* 257:209–221.

de Hoop, M., C. von Poser, C. Lange, E. Ikonen, W. Hunziker, and C.G. Dotti. 1995. Intracellular routing of wild-type and mutated polymeric immunoglobulin receptor in hippocampal neurons in culture. *J. Cell Biol.* 130:1447–1459.

Demyanenko, G.P., A.Y. Tsai, and P.F. Maness. 1999. Abnormalities in neuronal process extension, hippocampal development, and the ventricular system of L1 knockout mice. *J. Neurosci.* 19:4907–4920.

Dickson, T.L., C.D. Mintz, D.L. Benson, and S.R.J. Salton. 2002. Functional binding interaction identified between the axonal CAM L1 and members of the ERM family. *J. Cell Biol.* 157:1105–1112.

Dotti, C.G., and K. Simons. 1990. Polarized sorting of viral glycoproteins to the axon and dendrites of hippocampal neurons in culture. *Cell.* 62:63–72.

Folsch, H., H. Ohno, J.S. Bonifacino, and I. Mellman. 1999. A novel clathrin adaptor complex mediates basolateral targeting in polarized epithelial cells. *Cell.* 99:189–198.

Fourgeaud, L., A.S. Bessis, F. Rossignol, J.P. Pin, J.C. Olivo-Marin, and A. Hemar. 2003. The metabotropic glutamate receptor mGluR5 is endocytosed by a clathrin-independent pathway. *J. Biol. Chem.* 278:12222–12230.

Francesconi, A., and R.M. Duvoisin. 2002. Alternative splicing unmasks dendritic and axonal targeting signals in metabotropic glutamate receptor 1. *J. Neurosci.* 22:2196–2205.

Garrido, J.J., F. Fernandes, P. Giraud, I. Mouret, E. Pasqualini, M.P. Fache, F. Jullien, and B. Dargent. 2001. Identification of an axonal determinant in the C-terminus of the sodium channel Na(v)1.2. *EMBO J.* 20:5950–5961.

Jareb, M., and G. Banker. 1997. Inhibition of axonal growth by brefeldin A in hippocampal neurons in culture. *J. Neurosci.* 17:8955–8963.

Jareb, M., and G. Banker. 1998. The polarized sorting of membrane proteins expressed in cultured hippocampal neurons using viral vectors. *Neuron.* 20:855–867.

Kamiguchi, H., and V. Lemmon. 1998. A neuronal form of the cell adhesion molecule L1 contains a tyrosine-based signal required for sorting to the axonal growth cone. *J. Neurosci.* 18:3749–3756.

Kamiguchi, H., and V. Lemmon. 2000. Recycling of the cell adhesion molecule L1 in axonal growth cones. *J. Neurosci.* 20:3676–3686.

Kamiguchi, H., K.E. Long, M. Pendergast, A.W. Schaefer, I. Rapoport, T. Kirchhausen, and V. Lemmon. 1998. The neural cell adhesion molecule L1 interacts with the AP-2 adaptor and is endocytosed via the clathrin-mediated pathway. *J. Neurosci.* 18:5311–5321.

Klausner, R.D., J.G. Donaldson, and J. Lippincott-Schwartz. 1992. Brefeldin A: insights into the control of membrane traffic and organelle structure. *J. Cell Biol.* 116:1071–1080.

Luton, F., M.H. Cardone, M. Zhang, and K.E. Mostov. 1998. Role of tyrosine phosphorylation in ligand-induced regulation of transcytosis of the polymeric Ig receptor. *Mol. Biol. Cell.* 9:1787–1802.

Matter, K., W. Hunziker, and I. Mellman. 1992. Basolateral sorting of LDL receptor in MDCK cells: the cytoplasmic domain contains two tyrosine-dependent targeting determinants. *Cell.* 71:741–753.

Matter, K., E.M. Yamamoto, and I. Mellman. 1994. Structural requirements and sequence motifs for polarized sorting and endocytosis of LDL and Fc receptors in MDCK cells. *J. Cell Biol.* 126:991–1004.

Matter, K.M., J.A. Whitney, E.M. Yamamoto, and I. Mellman. 1993. Common signals control low density lipoprotein receptor sorting in endosomes and the Golgi complex of MDCK cells. *Cell.* 74:1053–1064.

Mellman, I. 1995. Molecular sorting of membrane proteins in polarized and nonpolarized cells. *Cold Spring Harb. Symp. Quant. Biol.* 60:745–752.

Mostov, K., T. Su, and M. ter Beest. 2003. Polarized epithelial membrane traffic: conservation and plasticity. *Nat. Cell Biol.* 5:287–293.

Mostov, K.E., and M.H. Cardone. 1995. Regulation of protein traffic in polarized epithelial cells. *Bioessays.* 17:129–134.

Ohno, H., T. Tomemori, F. Nakatsu, Y. Okazaki, R.C. Aguilar, H. Foelsch, I. Mellman, T. Saito, T. Shirasawa, and J.S. Bonifacino. 1999. Mu1B, a novel adaptor medium chain expressed in polarized epithelial cells. *FEBS Lett.* 449:215–220.

Sampo, B., S. Kaech, S. Kunz, and G. Banker. 2003. Two distinct mechanisms target membrane proteins to the axonal surface. *Neuron.* 37:611–624.

Scales, S.J., R. Pepperkok, and T.E. Kreis. 1997. Visualization of ER-to-Golgi transport in living cells reveals a sequential mode of action for COPII and COPI. *Cell.* 90:1137–1148.

Schaefer, A.W., Y. Kamei, H. Kamiguchi, E.V. Wong, I. Rapoport, T. Kirchhausen, C.M. Beach, G. Landreth, S.K. Lemmon, and V. Lemmon. 2002. L1 endocytosis is controlled by a phosphorylation–dephosphorylation cycle stimulated by outside-in signaling by L1. *J. Cell Biol.* 157:1223–1232.

Schmid, R.S., W.M. Pruitt, and P.F. Maness. 2000. A MAP kinase-signaling pathway mediates neurite outgrowth on L1 and requires Src-dependent endocytosis. *J. Neurosci.* 20:4177–4188.

Seeger, M., and G.S. Payne. 1992. Selective and immediate effects of clathrin heavy chain mutations on Golgi membrane protein retention in *Saccharomyces cerevisiae.* *J. Cell Biol.* 118:531–540.

Stowell, J.N., and A.M. Craig. 1999. Axon/dendrite targeting of metabotropic glutamate receptors by their cytoplasmic carboxy-terminal domains. *Neuron.* 22:525–536.

Tienari, P.J., B. De Strooper, E. Ikonen, M. Simons, A. Weidemann, C. Czech, T. Hartmann, N. Ida, G. Multhaup, C.L. Masters, et al. 1996. The beta-amyloid domain is essential for axonal sorting of amyloid precursor protein. *EMBO J.* 15:5218–5229.

Tuma, P.L., and A.L. Hubbard. 2003. Transcytosis: crossing cellular barriers. *Physiol. Rev.* 83:871–932.

van Ijzendoorn, S.C., M.J. Tuvim, T. Weimbs, B.F. Dickey, and K.E. Mostov. 2002. Direct interaction between Rab3b and the polymeric immunoglobulin receptor controls ligand-stimulated transcytosis in epithelial cells. *Dev. Cell.* 2:219–228.

Vogt, L., R.J. Giger, U. Ziegler, B. Kunz, A. Buchstaller, W.T.J.M.C. Hermens, M.G. Kaplitt, M.R. Rosenfeld, D.W. Pfaff, J. Verhaagen, and P. Sonderegger. 1996. Continuous renewal of the axonal pathway sensor apparatus by insertion of new sensor molecules into the growth cone membrane. *Curr. Biol.* 6:1153–1158.

Wandinger-Ness, A., M.K. Bennett, C. Antony, and K. Simons. 1990. Distinct transport vesicles mediate the delivery of plasma membrane proteins to the apical and basolateral domains of MDCK cells. *J. Cell Biol.* 111:987–1000.

West, A.E., R.L. Neve, and Y.K.M. Buckle. 1997. Identification of a somatodendritic targeting signal in the cytoplasmic domain of the transferrin receptor. *J. Neurosci.* 17:6038–6047.

Winckler, B., and I. Mellman. 1999. Neuronal polarity: controlling the sorting and diffusion of membrane components. *Neuron.* 23:637–640.

Winckler, B., P. Forscher, and I. Mellman. 1999. A diffusion barrier maintains distribution of membrane proteins in polarized neurons. *Nature.* 397:698–701.